SETAC PRESS

Environmental Toxicology and Chemistry, Vol. 24, No. 1, pp. 129–135, 2005

Printed in the USA
0730-7268/05 $12.00 + .00

UPTAKE AND DEPURATION OF PARALYTIC SHELLFISH TOXINS IN THE GREEN-LIPPED MUSSEL, *PERNA VIRIDIS*: A DYNAMIC MODEL

ASHLEY M.Y. LI,† PETER K.N. YU,‡ DENNIS P.H. HSIEH,§ WEN-XIONG WANG,§ RUDOLF S.S. WU,† and PAUL K.S. LAM*†

†Department of Biology and Chemistry, ‡Department of Physics and Materials Science, City University of Hong Kong, 83 Tat Chee Avenue, Kowloon, Hong Kong, People's Republic of China

§Department of Biology, The Hong Kong University of Science and Technology, Clear Water Bay, Hong Kong, People's Republic of China

(*Received* 14 *July* 2003; *Accepted* 16 *June* 2004)

Abstract—Uptake and depuration of paralytic shellfish toxins in the green-lipped mussel, *Perna viridis*, were investigated by exposing the mussels to dinoflagellates (*Alexandrium tamarense*, ACTI01) under laboratory conditions for 8 d, then depurating them in clean seawater for 14 d. First-order linear differential equations were set up for five tissue compartments: Viscera, gill, hepatopancreas, adductor muscle, and foot. The solutions to these equations were used to fit the experimental data. We then estimated the parameters governing the model, which depend on the elimination rate from each compartment and the transfer coefficient between compartments. An assumption of the model is that the gills transport the dinoflagellates directly to the mouth and then to the viscera, where the ingested cells are broken down, releasing the toxins. The toxins absorbed are transferred to other tissues. During the uptake phase, the transfer coefficients from viscera to gill, hepatopancreas, adductor muscle, and foot were 0.03, 0.24, 0.01, and 0.004 per day, respectively. During the depuration phase, the transfer coefficients were 0.01, 0, 0.01, and 0.003 per day, respectively. In terms of the anatomical distribution of *N*-sulfocarbamoyl-11-hydroxysulfate (C2) toxins in various tissues, viscera and hepatopancreas contained the highest percentages (47–74% and 8–41%, respectively). Together, these two tissue compartments accounted for 71 to 96% of all C2 toxins present. The biokinetic model allows a quantitative prediction of C2 toxins in whole mussel as well as individual tissue compartments based on the density estimates and toxin load of dinoflagellate cells in the surrounding waters over time.

Keywords—*Perna viridis* Paralytic shellfish toxins Uptake Depuration Dynamic model

INTRODUCTION

Harmful algal blooms that can cause paralytic shellfish poisoning (PSP) have attracted much attention in recent decades. Paralytic shellfish toxins (PSTs) are fast-acting neurotoxins that inhibit transmission of nerve impulses by blocking sodium channels. These toxins can result in death by respiratory arrest within a few minutes to a few hours [1]. Paralytic shellfish toxins can accumulate to very high concentrations in aquatic biota and biomagnify through the food chain. For these reasons, PSTs constitute an important health hazard to seafood consumers [2,3], particularly in countries lacking an effective surveillance system. Indeed, the occurrence of PSTs in shellfish has caused major economic losses to the aquaculture industries (millions of U.S. dollars, in some cases) of many countries [4,5].

Extensive research on PSP has been undertaken in North America, focusing mainly on the impacts of toxic dinoflagellates on commercially important shellfish species [5]. Considerable information now exists regarding the accumulation, depuration, and biotransformation of PSP toxins in North American shellfish; this provides a strong scientific basis for assessing and managing risks to the shellfish industry and seafood consumers.

In contrast to North America, the biokinetics of PSTs in commercially important species of the tropics are virtually unknown. The biochemical, physiological, and behavioral responses of shellfish to toxic dinoflagellates clearly are species- and site-specific [5], however, so the information derived from temperate shellfish is not directly applicable to tropical species.

The shellfish industry in many tropical countries has developed rapidly in recent decades. In China alone, the productivity of major shellfish species, such as scallops, mussels, oysters, and clams, has increased 20-fold from 1993 to 1996 [6]. Parallel to this trend, the number of incidents of seafood poisoning associated with PSTs in China has increased, particularly along the northern and southern coasts [7,8]. In 1986, one person died and 136 people became seriously ill in Dongshan county of Fujian Province because of the consumption of PST-contaminated clams, *Venerupis philippinarum* [6]. In 1991, two fatalities were reported as a result of the consumption of PST-laden green mussels, *Perna viridis*, from the shellfish aquaculture zone at Daya Bay, Guangdong Province, southern China. Lin et al. [9] analyzed the PST levels in 24 species of shellfish from Guangdong coast and reported that the scallop, *Chlamys nobilis*, and the mussel, *P. viridis*, were the most toxic species. The toxicity levels exceeded the World Health Organization health limit (4,000 MU kg^{-1}), and the shellfish were deemed to be unsuitable for human consumption.

In the South China Sea, the main PSP-causative organisms are dinoflagellates, such as *Alexandrium tamarense*, *A. catenella*, and *Gonyaulax polyedra* [6–10]. These species produce primarily the *N*-sulfocarbamoyl C toxins that have relatively low potency [11–13]. Indeed, the *N*-sulfocarbamoyl-11-hydroxysulfate toxin (C2) dominates the PST contamination of shellfish in this region [14].

Exponential decay equations have been used to calculate

* To whom correspondence may be addressed (bhpksl@cityu.edu.hk).

''detoxification'' rates of various bivalve species (see [5] and references therein). Recently, similar exponential decay models were used by Blanco et al. [15] to describe the depuration kinetics of amnesic shellfish poisoning toxin, domoic acid, in the king scallop, *Pecten maximus*. However, complete dynamic models derived from first principles have not been constructed for the biokinetics of PSTs. It is instructive to explore the use of such dynamic models to quantitatively describe the transfer of toxins from toxigenic algae into the mussel and between different tissue compartments of the mussel. These types of models allow quantitative prediction of PST levels in the whole animal and in individual tissue compartments based on density estimates and toxin load of the algal cells over time.

The green-lipped mussel, *Perna viridis* (Linnaeus, 1758) (Bivalvia: Mytilacea), is widely distributed in tropical/subtropical Asia and is an important culture species in China and Southeast Asian countries, such as the Philippines, India, Singapore, and Thailand [16]. Although a postcolumn high-performance liquid chromatography (HPLC) derivatization coupled with fluorescence detection is very useful in the separation and analysis of PSTs, it is less effective for shellfish surveillance in routine monitoring situations, because the method involves a time-consuming solid-phase extraction procedure and requires three independent isocratic runs for the separation of C toxins, gonyautoxins (GTX), neosaxitoxin (neoSTX), and saxitoxin (STX).

The present study aims to investigate the uptake and depuration dynamics of PSTs in *P. viridis* exposed to toxin-laden dinoflagellates (*A. tamarense*, ACTI01) under laboratory conditions and to construct a biokinetic model for PSTs in the mussel that allows a quantitative prediction of PST levels in the whole animal as well as individual tissue compartments from the density and toxin content of dinoflagellate cells over time. First-order linear differential equations were established for five tissue compartments in the mussel: Viscera, gill, hepatopancreas, adductor muscle, and foot. The solutions to the five equations then are used to fit the experimental data. The parameters governing the biokinetic model, which depend on the elimination rate from each compartment and the transfer coefficient between compartments, are estimated. Information on PST levels in the shellfish, as predicted by the biokinetic model using data from an effective monitoring program on toxigenic dinoflagellates, is used to provide a scientific basis for a cost-effective assessment and management of PSP-associated risks.

MATERIALS AND METHODS

Mussel exposure and depuration experiments

Green-lipped mussels (*P. viridis*) with shell lengths between 8 and 10 cm were collected from a fish farm at Kat O (Hong Kong, China) and transported to the laboratory, where fouling organisms were removed from the exterior of the shells. The mussels were acclimated in clean seawater (obtained from Ocean Park, Hong Kong, China) for 7 d. To start the experiment, 22 mussels were placed into each of five glass tanks (2 L of seawater per mussel) under a 16:8-h light:dark cycle. The mussels were exposed to a single toxigenic alga, *A. tamarense* (ACTI01), for 8 d and then put back in clean seawater to depurate for another 14 d. Seawater used in all experiments was maintained at 21–23°C. The mussels in each tank were inspected for mortality daily. Fifteen mussels died over the experimental period and were removed. Previous observations indicate that such mortality rates are not unusual even under clean-water conditions.

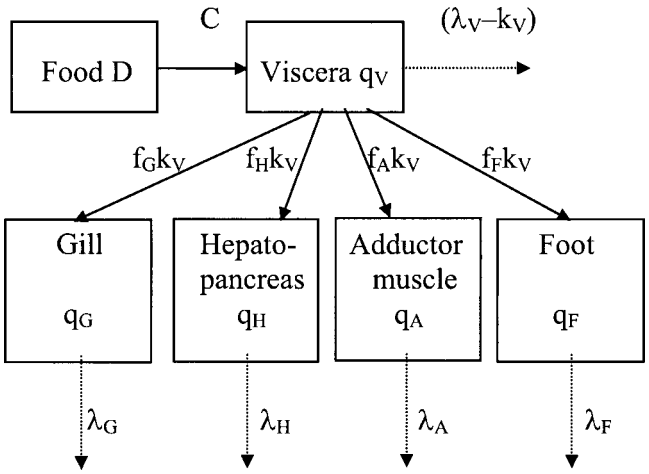

Fig. 1. Schematic for the five compartments of *Perna viridis*: Gill, viscera, hepatopancreas, adductor muscle, and foot. The $f_G k_V$, $f_H k_V$, $f_A k_V$, and $f_F k_V$ terms are the transfer coefficients from viscera to other compartments (solid lines). The λ_G, λ_H, λ_A, and λ_F terms are the removal rates from various compartments (dotted lines). Other parameters used in compartment scheme are given in Table 1.

The ACTI01 strain was derived from a single cyst isolated from sediments collected from Dapeng Bay (Shenzhen, China) in 1992 [17]. Subcultures of *A. tamarense* were maintained in natural seawater with sterilized K-medium in 2-L conical flasks. Natural seawater was passed through a 0.45-μm nylon membrane filter and autoclaved at 120°C for 15 min before use. Large-scale culture was conducted in 30-L glass tanks inside an environmental chamber maintained at 21–23°C with an average light intensity of 5,000 lux and a 14:10-h light: dark cycle. The cultures were well aerated with spherical air stones after filtration through disposal syringe filters with a pore size of 0.20 μm. Seawater containing *A. tamarense* at a cell density of 1.5×10^5 cells/ml was used for the first 8 d; seawater only was used for the remaining 14 d. The medium was changed daily while maintaining a constant volume (2 L) of seawater per mussel. Every 2 d, one mussel was removed randomly from each tank for analysis to minimize possible tank effects, so each treatment had five replicates. Each sampled mussel was dissected into five body compartments (hepatopancreas, gill, foot, adductor muscle, and viscera). The tissues were stored at −20°C until analyzed.

Toxin extraction

Each day, 20 ml of the *Alexandrium* culture were removed from each tank. A 10-ml volume of the culture was used for toxin extraction; the other 10-ml volume was used for cell counting. Algal cells were harvested by centrifugation at 2,200 *g* for 10 min. The cell pellet was resuspended in 0.5 ml of 50 mM acetic acid. Toxin extraction from the cells was facilitated by an ultrasonic probe (High Intensity Ultrasonic Processor: An Auto-Tune Series; Sonics, Danbury, CT, USA) with the power set to 30 W for 15 s, followed by centrifugation of the homogenate at 19,283 *g* for 10 min at 4°C. A 10-μl volume of the supernatant was injected into the HPLC for toxin quantification.

For the mussel tissues, the samples were first defrosted at 4°C, then homogenized with 50 mM acetic acid (1:1 fresh wt: acid). The samples were further homogenized with an ultra-

Table 1. Parameters used in the compartment scheme shown in Figure 1[a]

Parameter	Description	Unit
C	(mg of toxin into viscera per d) per (pg per mg of toxin in food)	pg/d
$f_G f_V$	Transfer coefficient from viscera to gill	per d
$f_H k_V$	Transfer coefficient from viscera to hepatopancreas	per d
$f_A k_V$	Transfer coefficient from viscera to adductor muscle	per d
$f_F k_V$	Transfer coefficient from viscera to foot	per d
q_i	pg mg^{-1} of toxin in the i-th compartment	pg/mg
m_i	Wet mass of the i-th compartment	mg
λ_i	Removal rate from the i-th compartment	per d

[a] i = V, G, H, A, and F represents the compartments of viscera, gill, hepatopancreas, adductor muscle, and foot, respectively.

sonic probe, then centrifuged at 19,283 *g* for 10 min to obtain a clear supernatant. The toxin-containing supernatant was purified by passing it through a reversed-phase cartridge column (C18 Sep-Pak; Waters, Milford, MA, USA) that had been preconditioned with 20 ml of MilliQ water (Millipore, Bedford, MA, USA) before being equilibrated with 50 mM acetic acid. The extract was loaded into the column. The column's eluent and 0.5 ml of 50 mM acetic acid wash were collected. A volume of 10 to 15 μl of the purified extract was injected into the HPLC for PST determination.

Toxin analyses

The toxins analyzed in the present study included C2, GTX1 through GTX4, neoSTX, and STX. The analytical procedures followed those described by Oshima [18], which involved a postcolumn derivatization coupled with fluorescence detection. The HPLC system was from Waters. A stainless-steel column containing reverse-phase packing (Inertsil C8 [film thickness, 3 μ; length, 150 mm; inner diameter, 4.6 mm] and Inertsil C8 [film thickness, 5 μ; length, 7.5 mm; inner diameter, 4.6 mm] all-guard cartridges; Alltech, Deerfield, IL, USA) was used.

We used 7 mM periodic acid in 50 mM potassium phosphate buffer (pH 9.0) as the oxidizing reagent, and 0.5 M acetic acid was used as the acidifying reagent. To optimize separation of the toxins, we used an isocratic elution with three mobile phases. Briefly, 1 mM tetrabutyl ammonium phosphate (pH 5.8) was used for C2 toxin, 2 mM sodium 1-heptanesulfonate in 10 mM ammonium phosphate (pH 7.1) for GTX1 through GTX4, and 2 mM sodium 1-heptanesulfonate in 30 mM ammonium phosphate (pH 7.1) for neoSTX and STX [18]. The STX, neoSTX, GTX1/4, and GTX2/3 standards (National Research Council of Canada, Halifax, NS, Canada) were used for toxin verification. The C2 toxin standard was kindly provided by Y. Oshima and was reconfirmed using purified C2 toxin that we produced.

The detection limits for the individual toxins were as follows: C2, 12 ng; STX, 0.08 ng; neoSTX, 1 ng; GTX1, 17 ng; GTX2, 4 ng; GTX3, 4 ng; and GTX4, 10 ng. Analyses generally differed by less than 10%. Percentage recovery values of 60 to 72% were estimated for the dominant toxin, C2. Toxin concentrations were not corrected for recovery rates.

Model

The model we developed assumes that the gills of *P. viridis* retain and transport the dinoflagellates along external food grooves to the mouth and the viscera. Thus, the toxins move from the ingested dinoflagellate cells to the viscera. The algal cells are broken down in the viscera, where the released toxins can be absorbed. The toxins are then transferred to the other tissue compartments (i.e., gills, hepatopancreas, adductor muscle, and foot). Another assumption is that the loss of toxins during the depuration phase is achieved predominantly by transferal from the four tissue compartments to seawater. Two-compartment models generally use the viscera as the first compartment, and the remaining tissues (e.g., gills, adductor muscles, and foot) are pooled to form the second compartment (see [5] and references therein). In the present study, the viscera, gill, hepatopancreas, adductor muscle, and foot of *P. viridis* were modeled by five compartments, and the biokinetics were modeled by first-order linear differential equations. A schematic of the five compartments is shown in Figure 1. Parameters used in the compartment scheme (i = V, G, H, A, and F represents the compartments of viscera, gill, hepatopancreas, adductor muscle, and foot, respectively) are listed

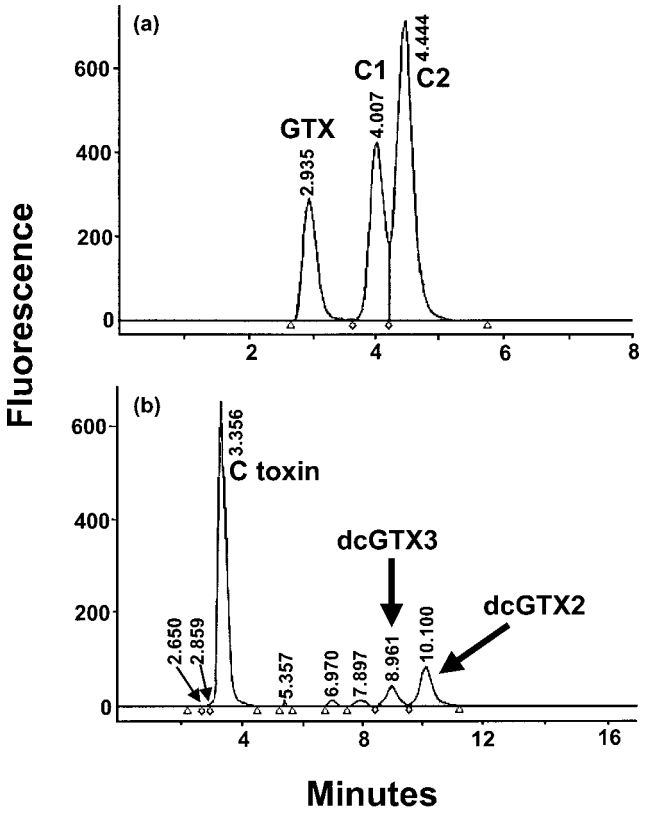

Fig. 2. Typical chromatograms of paralytic shellfish toxins (C, gonyautoxins [GTX], and dcGTX toxins) in tissue extracts. (**a**) 1 mM tetrabutyl ammonium phosphate (pH 5.8) for C toxin. (**b**) 2 mM sodium 1-heptanesulfonate in 10 mM ammonium phosphate (pH 7.1) for GTX toxins.

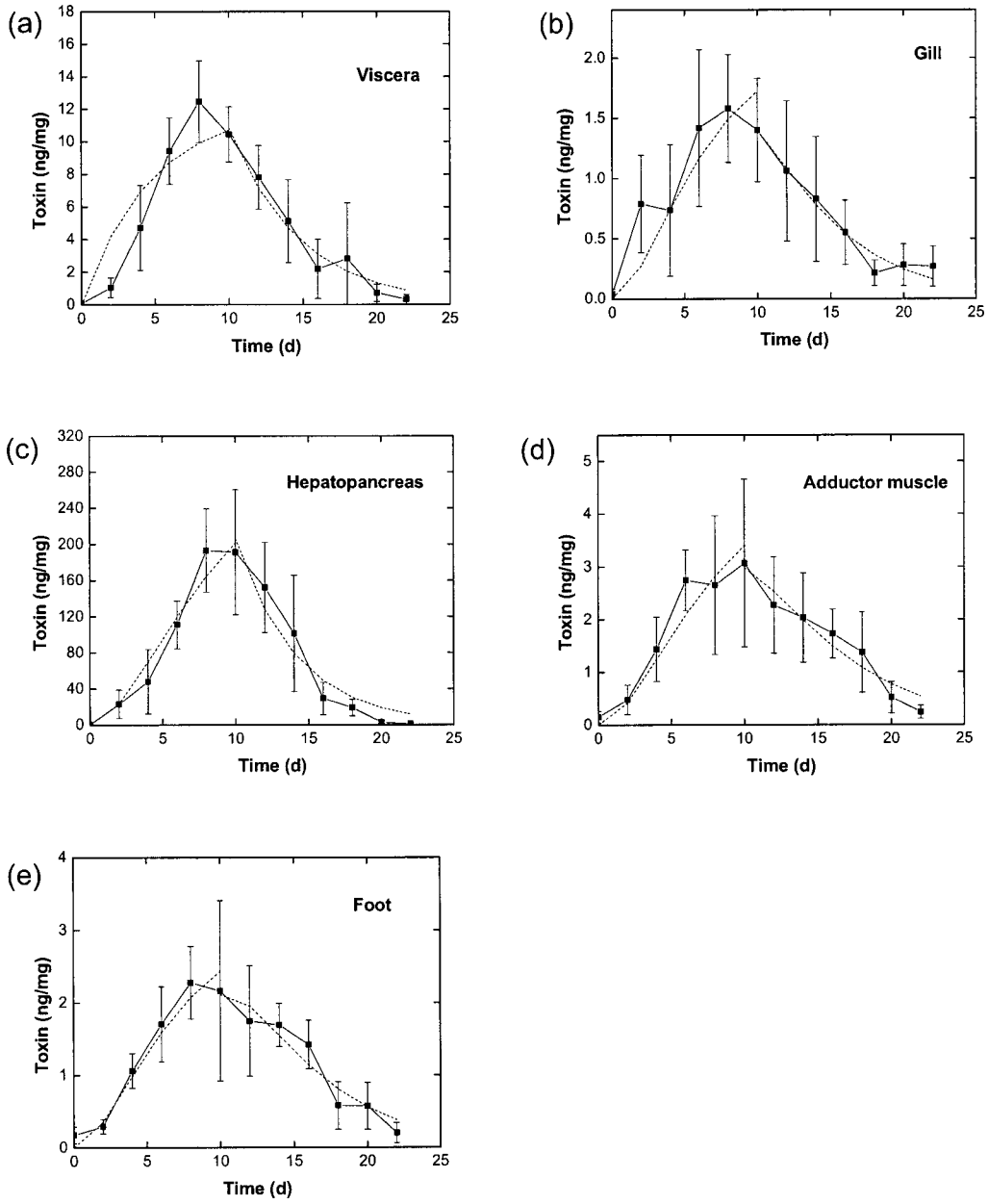

Fig. 3. Concentration (ng/mg) of toxin at different culture times in (**a**) viscera, (**b**) gill, (**c**) hepatopancreas, (**d**) adductor muscle, and (**e**) foot of *Perna viridis*. Dotted line indicates best fit. Depuration started on the 10th day. Vertical lines represent ± one standard deviation ($n = 5$).

in Table 1. The toxin concentration in the food (pg/mg) is denoted as D. The equations governing the biokinetics and the time-dependent toxin concentrations in each of the five compartments are given below.

Differential equations governing the biokinetics for the viscera are as follows: For uptake,

$$\text{Uptake:} \quad \frac{dq_V}{dt} = \frac{CD}{m_V} - \lambda_V q_V \tag{1}$$

$$\text{Depuration:} \quad \frac{dq_V}{dt} = -\lambda_V q_V \tag{2}$$

The differential equation governing the biokinetics during uptake and depuration for the other compartments (j = G, H, A, and F) is

$$\frac{dq_j}{dt} = \frac{m_V}{m_j} f_j k_V q_V - \lambda_j q_j \tag{3}$$

Time-dependent toxin concentrations in each compartment during uptake with the initial conditions $q_V(0) = q_j(0)$ are as follows:

$$q_V = \frac{CD}{m_V \lambda_V}(1 - e^{-\lambda_V t}) \tag{4}$$

$$q_j = \frac{f_j k_V CD}{\lambda_V m_i}\left[\left(\frac{1 - e^{-\lambda_j t}}{\lambda_j}\right) + \left(\frac{e^{-\lambda_j t} - e^{-\lambda_V t}}{\lambda_j - \lambda_V}\right)\right] \tag{5}$$

where CD is the amount of toxin taken into the viscera from food (per d), $f_j k_V$ is the transfer coefficient from viscera to other tissue compartments (per d), and λ_j is the removal rate from compartment j (per d).

Time-dependent toxin concentrations in each of the five compartments during depuration with the initial conditions (on day 10) $q_V(0) = q_{Vo}$ and $q_j(0) = q_{jo}$ are as follows:

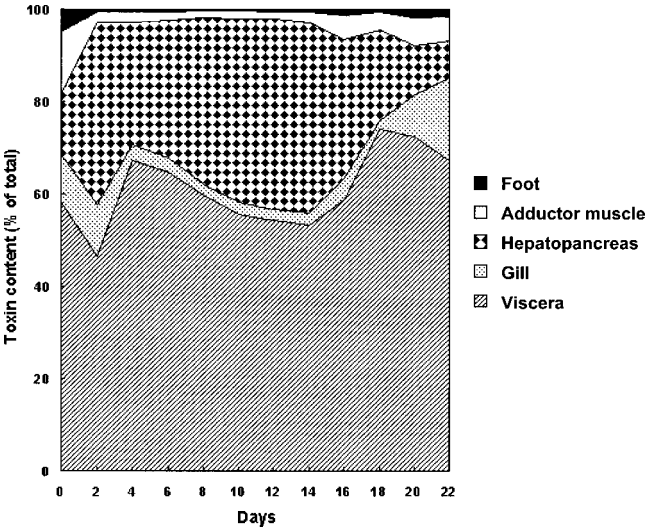

Fig. 4. Anatomical distribution (% total toxin content) of *N*-sulfocarbamoyl-11-hydroxysulfate toxins in the viscera, gill, hepatopancreas, adductor muscle, and foot of *Perna viridis* throughout the experimental period (days 0–8, uptake; days 9–22, depuration).

$$q_V = q_{Vo}e^{-\lambda_V t} \quad (6)$$

$$q_j = q_{jo}e^{-\lambda_j t} + \frac{m_V}{m_j} f_j k_V q_{Vo} e^{-\lambda_V t}\left(\frac{e^{-\lambda_V t} - e^{-\lambda_j t}}{\lambda_j - \lambda_V}\right) \quad (7)$$

Therefore, if k_V, λ_V, λ_G, λ_H, λ_A, λ_F, and *CD* are determined, the biokinetics of the toxin in all the five compartments of *P. viridis* can be calculated.

RESULTS

Toxin distribution

The present study analyzed C2, GTX1 through GTX4, neoSTX, and STX. Typical chromatograms of the PSTs analyzed are shown in Figure 2. Our analyses revealed that the local *A. tamarense* strain (ACTI01) produced PSTs comprising more than 98% C2 toxins, with trace amounts of GTX3. In the tissue of the mussels exposed to *A. tamarense* (ACTI01), approximately 80% of the PSTs found were C2 toxins; GTX1, GTX3, and GTX4 accounted for the bulk of the remaining toxins. Previous studies suggest that attention should be focused on C2 toxins, which dominate the PST contamination of local shellfish [14,17]. This finding justifies the use of C2 toxins in modeling the biokinetics of PSTs in *P. viridis* in the present study.

On day 0, the toxin levels in all five compartments were generally low (near zero) (Fig. 3). Exposure to *A. tamarense* cells resulted in a steady increase in toxin levels in all body compartments. The data shown in Figure 3 exhibit some variability (mean ± standard error, 52.8% ± 3.5%). Given that repeatability of the analytical method used was less than 10%, variations in the uptake data probably resulted from the different pathways/processes involved in the uptake of the toxins (e.g., ingestion of the algae or, to a lesser extent, direct absorption of dissolved toxins, followed by the digestion of algal cells and assimilation of toxins). Transfer of the mussels to toxin-free seawater resulted in a marked decrease in toxin levels in all tissue compartments; this response was delayed in the hepatopancreas and adductor muscle (Fig. 3). After 10 to 12 d, all compartments were effective in depurating the toxins and attaining levels near those at the start of the dosing experiment (Fig. 3).

In terms of the anatomical distribution of C2 toxins, viscera and hepatopancreas contained the greatest percentages, ranging from 47 to 74% and 8 to 41%, respectively (Fig. 4). Together, these two tissue compartments accounted for 71 to 96% of all C2 toxins in the mussel throughout the experiment (Fig. 4). Percentages of toxin contents in the gill, adductor muscle, and foot remained low and relatively stable, ranging from 2 to 18%, 1 to 13%, and 0.4 to 5%, respectively (Fig. 4).

Model fitting

The experimental data were fitted using user-defined expressions in the nonlinear curve fit program of the Microcal™ Origin™ software (Ver 6.0; OriginLab, Northampton, MA, USA) with the parameters of interest as the user-defined parameters [16]. The weights of different parts of *P. viridis* were also measured (Table 2).

Viscera. From the depuration data in Figure 3, the fitted curve gives the following results:

$$q_{Vo} = 10{,}900 \pm 700 \text{ (pg/mg)}$$

$$\lambda_V = 0.21 \pm 0.02 \text{ (per d)}$$

Using λ_V to fit the uptake data, we found that *CD* = 16,741 (ng/d). We used these values to fit the data for the other compartments.

Gill. From the depuration data in Figure 3, the fitted curve gave the following results:

$$q_{Go} = 1400 \pm 100 \text{ (pg/mg)}$$

$$\lambda_G = 0.45 \pm 0.45 \text{ (per d)}$$

$$f_G k_V = 0.01 \text{ (per d)}$$

Using λ_G and the above *CD* values to fit the uptake data, we found that $f_G k_V = 0.03$ (per d).

Hepatopancreas, adductor muscle, and foot. Using similar derivation methods, corresponding parameters were estimated for hepatopancreas, adductor muscle, and foot. A summary of the fitted parameters is given in Table 3.

DISCUSSION

When placed in toxin-free seawater, all tissue compartments of *P. viridis* were effective in depurating the toxins and attaining levels near those that occurred at the start of the dosing experiment. Indeed, Bricelj and Shumway [5] considered mussels to be quick detoxifiers, with an ability to remove most accumulated toxins within a few weeks. In terms of the anatomical distribution of C2 toxins, viscera and hepatopancreas contained the greatest percentages. These two tissue com-

Table 2. Measured weights of different compartments of *Perna viridis* (n = 10)[a]

	Viscera	Gill	Hepatopancreas	Adductor muscle	Foot
Wet weight (g)	6.54 ± 0.53	2.08 ± 0.15	0.26 ± 0.09	0.71 ± 0.09	0.23 ± 0.04

[a] Values are presented as the mean ± standard deviation.

Table 3. Summary of the fitted parameters[a]

	Viscera	Gill	Hepatopancreas	Adductor muscle	Foot
q_o (ng/mg)	10.9 ± 0.7	1.4 ± 0.1	206 ± 20	3 ± 0.3	2 ± 0.2
λ (per d)	0.21 ± 0.02	0.45 ± 0.45	0.24 ± 0.04	0.28 ± 0.21	0.38 ± 0.24
$(f_j k_V)_{uptake}$ (per d)	NA[b]	0.03	0.24	0.01	0.004
$(f_j k_V)_{depuration}$ (per d)	NA	0.01	0	0.01	0.003

[a] Values are presented as the mean ± standard error, with $n = 6$ for the uptake phase and $n = 7$ for the depuration phase.
[b] NA = not applicable.

partments together accounted for 71 to 96% of all the C2 toxins present in the mussel. The digestive processes that occur in the viscera are important in releasing toxins by rupturing the dinoflagellate cell walls. Taking into account the relatively small mass of the hepatopancreas, the relatively high concentrations of toxins in this compartment suggest that the hepatopancreas is the major site for toxin deposition and, probably, for detoxification in mussels. The gill, adductor muscle, and foot did not accumulate toxins much, but they may have facilitated the transfer of toxins to other tissues. Similar low levels of toxins have been found in the gill, adductor muscle, and foot of a range of bivalves [5,19,20]. Overall, the anatomical distribution patterns of C2 toxins in *P. viridis* were consistent with those of other bivalve species reviewed in Bricelj and Shumway [5].

In addition,

$$\sum_j f_j k_V = 0.28 \text{ during uptake,} \tag{8}$$

which is near the λ_V of 0.21 ± 0.024, suggesting that all the toxins had been effectively removed from the viscera compartment by transferal to other compartments during the uptake stage. The observation that

$$\sum_j f_j k_V = 0.024 \tag{9}$$

during depuration, which is much smaller than the λ_V, suggests that almost all the toxins had been eliminated during the depuration stage. Whereas $f_j k_V$ did not vary much during the uptake and depuration stages for the gill, adductor muscle, and foot, it declined from a high value to zero for the hepatopancreas. Thus, depuration of toxins from the mussel occurred principally via a loss of toxins from the hepatopancreas when the animal was placed into toxin-free seawater. Our model clearly shows that the transfer of toxins into and out of the mussel occurs almost completely via two specific tissue compartments: Viscera, and hepatopancreas. Toxin removal rates (λ) for viscera and hepatopancreas were 0.21 and 0.24 per d, respectively, with corresponding coefficient of variation values of 25 and 43%.

One- or two-compartment exponential decay models have been adopted for the depuration of toxins in the soft tissue of mussels (see [5] and references therein). However, the validity of such an assumption is rarely checked. Because the present model is derived from first principles, the validity of the assumptions involved can be investigated. For example, if the soft tissue of the mussel is treated as a single compartment (assuming that the soft tissue is made of the five compartments), then the concentration q_T of the tissue (with mass = m_T) can be written as

$$q_T = \frac{\sum m_i q_i}{\sum m_i} = \frac{m_V q_V + \sum m_j q_j}{m_T} \tag{10}$$

where q_V and q_j are given in Equation 6. Because the values of $f_j k_V$ are usually very small (the largest being only 0.01445, for the gill), the transferal term from the viscera to the j-th compartment during depuration is negligible compared to q_V. Therefore, Equation 10 can be simplified to

$$q_T \approx \frac{\sum m_i q_{i0} e^{-\lambda_i t}}{m_T} \tag{11}$$

From Figure 4, we notice that $m_V q_{V0} \gtrsim m_H q_{H0} \gg m_G q_{G0} \gtrsim m_A q_{A0} \gg m_F q_{F0}$, so further simplification is possible:

$$q_T \approx \frac{m_V q_{V0} e^{-\lambda_V t} + m_H q_{H0} e^{-\lambda_H t}}{m_T} \tag{12}$$

Incidentally, $\lambda_V \approx \lambda_H$ (0.21~0.24 d^{-1}). By replacing λ_V and λ_H with λ_T, we have

$$q_T \approx \left(\frac{m_V q_{V0} + m_H q_{H0}}{m_T}\right) e^{-\lambda_T t} \tag{13}$$

Thus, the depuration can be approximated by the exponential decay model from a single compartment, with the removal rate of approximately 0.22 per day. Chen and Chou [21] estimated a removal rate of 0.09 per day for the purple clam, *Hiatula rostrata*, whereas Bricelj and Shumway [5] reported toxin elimination rates of 5 to 15% per day for the blue mussel, *Mytilus edulis*, and 9 to 18% per day for the oyster, *Crassostrea iridescens*. This approximation is valid only when the toxin levels in the soft tissue are dominated by those in the viscera and hepatopancreas and these two compartments have similar removal rates.

It appears that the transfer of PSTs from toxic dinoflagellates into the mussel, the distribution of toxins in different body compartments, and the loss of toxins from the animal can be effectively modeled by first-order linear differential equations. The most important route of accumulation of phycotoxins in bivalves is through the ingestion of toxic phytoplankton [3]. The model used in the present study assumes that uptake of toxigenic algal cells as the dominant source of toxins and instantaneous and homogeneous distribution of toxins within each body compartment. It further assumes that the dominant process of toxin uptake is diffusion, which is a function of the diffusion coefficient and the concentration gradient of the toxins across exchange surfaces between body compartments. Using this biokinetic model, quantitative predictions on the uptake and depuration dynamics of PSTs in *P. viridis* as well as the transfer of these toxins between different body compartments of the shellfish can be made provided that the exposure profile (i.e., density of and toxin load in toxigenic algae over the exposure period) is known. Our results indicate that the toxin load of the algal cells is fairly stable and that daily density estimates are sufficient for modeling purposes. Such models can be constructed for a wide variety of temperate and tropical shellfish. In particular, the information on the

anatomical partitioning of toxins in different body compartments is especially relevant, because only specific body parts (e.g., the adductor muscle) are consumed in certain shellfish [22,23]. The biokinetic model developed here makes it possible to calculate PST concentrations in individual tissue compartments as well as the whole mussel based on estimates of the density and toxin load of the dinoflagellates in the water over time. This information about predicted toxin levels in shellfish provides a scientific basis for assessing and managing PSP-associated risks: It should facilitate management decisions on closing and reopening shellfish beds during and after toxic algal blooms, especially in tropical regions, for which relevant data are scarce.

The model proposed here was constructed using experimental data collected under controlled laboratory conditions. Thus, it may have some limitations. For example, the uptake and depuration patterns and rates may be influenced by abiotic/biotic variables, such as temperature and health of the animals. Even so, PSP occurrence in southern China follows a distinct, seasonal pattern, with peak levels being observed in the early spring (March and April), when temperatures typically range between 20 and 25°C. In the present study, the uptake and depuration experiments were performed at 22°C to simulate the conditions during bloom periods in the field. Models based on laboratory conditions lack some environmental realism, but the approach adopted in the present study generates a model that can predict toxin burdens in mussels. Thus, it enables a preliminary assessment of potential risks. As an example, it is possible to undertake risk assessment based on a worst-case scenario by assuming maximum toxin burden in the dinoflagellate cells, maximum uptake rates, and minimum depuration rates. If the risks under the worst-case scenario are still acceptable (i.e., toxin concentrations in mussels are less than the threshold levels), then no immediate management action would be needed. The biokinetic model developed here may benefit from validation and refinement using data derived from field-based studies.

Acknowledgement—The present study was supported by a Central Allocation Grant (8730020) and an Earmarked Research Grant (CityU1103/00M) awarded by the Research Grants Council, Hong Kong. We thank Monica Bricelj for her very valuable advice at the inception stage of this work. We also thank John Giesy for fruitful discussions on statistics.

REFERENCES

1. Duy TN, Lam PKS, Shaw G, Connell DW. 2000. Toxicology and risk assessment of freshwater cyanobacterial (blue-green algal) toxins in water. *Rev Environ Contam Toxicol* 163:113–186.
2. World Health Organization. 1984. Aquatic (marine and freshwater) biotoxins. Environmental Health Criteria 37. Geneva, Switzerland.
3. Moroño A, Franco J, Miranda M, Reyero MI, Blanco J. 2001. The effect of mussel size, temperature, seston volume, food quality, and volume-specific toxin concentration on the uptake rate of PSP toxin by mussels (*Mytilus galloprovincialis* Lmk). *J Exp Mar Biol Ecol* 257:117–132.
4. Chen CY, Chou HN. 1998. Transmission of the paralytic shellfish poisoning toxins, from dinoflagellate to gastropod. *Toxicon* 36: 515–522.
5. Bricelj MV, Shumway SE. 1998. Paralytic shellfish toxins in bivalve mollusks: Occurrence, transfer kinetics, and biotransformation. *Rev Fish Sci* 6:315–383.
6. Wang L, Li X. 1998. Management of shellfish safety in China. *J Shellfish Res* 17:1609–1611.
7. Zhou M, Li J, Luckas B, Yu R, Yan T, Hummert C, Kastrups S. 1999. A recent shellfish toxin investigation in China. *Mar Pollut Bull* 39:331–334.
8. Anderson DM, Kulis DM, Qi YZ, Zheng L, Lu S, Lin YT. 1996. Paralytic shellfish poisoning in Southern China. *Toxicon* 34:579–590.
9. Lin Y, Yang M, Chen R, Hu S, Jin G. 1994. Study on paralytic shellfish poison in shellfish from Guangdong coast. *Oceanologia et Limnologia Sinica* 25:220–225(in Chinese with English abstract).
10. Anderson DM, Andersen P, Bricelj VM, Cullen JJ, Hodgkiss IJ, Ho KC, Rensel JE, Wong JTY, Wu R. 1999. Red Tide—HAB monitoring and management in Hong Kong. Final Report. Agriculture and Fisheries Department, Hong Kong, China, p 262.
11. Oshima Y, Sugino K, Itakura H, Hirota M, Yasumoto T. 1990. Comparative studies on paralytic shellfish toxin profile of dinoflagellates and bivalves. In Graneli E, Sundstrom B, Edler L, Anderson DM, eds, *Toxic Marine Phytoplankton*. Elsevier Science, New York, NY, USA, pp 391–396.
12. Bricelj VM, Lee JH, Cembella AD. 1991. Influence of dinoflagellate cell toxicity on uptake and loss of paralytic shellfish toxins in the northern quahog, *Mercenaria mercenaria*. *Mar Ecol Prog Ser* 74:33–46.
13. Anderson DM, Kulis DM, Doucette GJ, Gallagher JC, Balech E. 1994. Biogeography of toxic dinoflagellates in the genus *Alexandrium* from the northeastern United States and Canada. *Mar Biol* 120:467–478.
14. Mak KCY, Li AMY, Hsieh DPH, Wong PS, Lam MHW, Wu RSS, Richardson BJ, Lam PKS. 2003. Paralytic shellfish toxins in green-lipped mussels, *Perna viridis*, in Hong Kong. *Mar Pollut Bull* 46:258–263.
15. Blanco J, Acosta CP, Bermúdez de la Puente M, Salgado C. 2002. Depuration and anatomical distribution of the amnesic shellfish poisoning (ASP) toxin domoic acid in the king scallop *Pecten maximus*. *Aquat Toxicol* 60:111–121.
16. Yu KN, Lam PKS, Ng KP, Li AMY. 2000. Biokinetics of cesium in *Perna viridis*. *Environ Toxicol Chem* 19:271–275.
17. Wang DZ, Hsieh DPH. 2001. Dynamics of C2 toxin and chlorophyll-*a* formation in the dinoflagellate *Alexandrium tamarense* during large-scale cultivation. *Toxicon* 39:1533–1536.
18. Oshima Y. 1995. Postcolumn derivatization liquid chromatography method for paralytic shellfish toxins. *JAOAC Int* 78:528–532.
19. Shimizu Y, Yoshioka M. 1981. Transformation of paralytic shellfish toxins as demonstrated in scallop homogenates. *Science* 212: 547–549.
20. Shumway SE, Sheman-Caswell S, Hurst JW Jr. 1988. Paralytic shellfish poisoning in Maine: Monitoring a monster. *J Shellfish Res* 7:643–652.
21. Chen CY, Chou HN. 2001. Accumulation and depuration of paralytic shellfish poisoning toxins by purple clam *Hiatula rostrata* Lightfoot. *Toxicon* 39:1029–1034.
22. Beitler MK. 1991. Toxicity of adductor muscles from the purple hinge rock scallop (*Crassadoma gigantea*) along the Pacific coast of North America. *Toxicon* 29:889–894.
23. Shumway SE, Cembella AD. 1993. The impact of toxic algae on scallop culture and fisheries. *Rev Fish Sci* 1:121–150.